RESEARCH ARTICLE
SPACE PHYSICS: MAGNETOSPHERIC PHYSICS

Earth and Planetary Physics
8: 215–221, 2024
doi: 10.26464/epp2023087

Origins of perturbations in dayside equatorial ground magnetograms

Syau-Yun W. Hsieh[1*], and David G. Sibeck[2]

[1]The Johns Hopkins University Applied Physics Laboratory, Laurel, Maryland, USA;

[2]NASA Goddard Space Flight Center, Greenbelt, Maryland, USA

Key Points:

- Increases in solar wind pressure increase dayside magnetospheric magnetic field strengths and cause northward perturbations in dayside equatorial ground magnetograms.
- Southward IMF turnings decrease dayside magnetospheric magnetic field strengths but are also associated with northward perturbations in dayside equatorial ground magnetograms.
- Solar wind pressure and southward IMF B_z turnings produce similar numbers of perturbation events in dayside equatorial ground magnetograms.

Citation: Hsieh, S-Y. W., and Sibeck, D. G. (2024). Origins of perturbations in dayside equatorial ground magnetograms. *Earth Planet. Phys.*, *8*(1), 215–221. http://doi.org/10.26464/epp2023087

Abstract: To determine the cause(s) of perturbations seen in dayside equatorial ground magnetograms, we conducted a systematic survey of simultaneous ground-based and geosynchronous satellite-based observations during the 90-day period from December 1, 2020 to February 28, 2021. We examined Huancayo ground magnetometer observations from 14:00:00 to 20:00:00 UT each day, during which Huancayo passed through local noon. From those data we chose perturbation events selected on the basis of large (>20 nT) event amplitude and classified the selected events as responding primarily to solar wind pressure, or to variations in the north/south component of the interplanetary magnetic field (IMF B_z), or perhaps in part to both. The results show that an equivalent number of events were identified for each model during this 90-day period. Variations in the lagged solar wind dynamic pressure routinely correspond to nearly simultaneous sudden impulses recorded at both geosynchronous orbit and on the ground. Variations in IMF B_z produce erosion signatures at geosynchronous orbit and can correspond to ground events if lag times for reconnection to enhance convection in the magnetosphere are taken into account.

Keywords: dayside magnetosphere; dayside equatorial ionosphere; geosynchronous magnetic field

1. Introduction

The Solar wind Magnetosphere Ionosphere Link Explorer (SMILE) is a stand-alone joint mission between the European Space Agency and the Chinese Academy of Sciences to study the global response of the magnetosphere to varying solar wind conditions (Branduardi-Raymont et al., 2018; Branduardi-Raymont and Wang C, 2022). SMILE has three objectives: (1) determine the fundamental modes of dayside solar wind-magnetosphere interaction, (2) define the substorm cycle, and (3) understand CME-driven storms and their relationship to substorms. SMILE addresses these tasks by taking observations of the soft X-rays generated by charge exchange in the magnetosheath and cusps, and by taking observations of far ultraviolet emissions from the auroral oval.

To address objective (1), SMILE identifies and tracks the locations of the magnetopause and cusps. Southward IMF turnings initiate reconnection on the dayside equatorial magnetopause, enabling its earthward erosion. By identifying, in soft X-ray observations, when, where, and how fast the magnetopause moves, and/or when and where the dayside auroral oval moves and brightens, researchers can determine where reconnection occurs and whether it is steady or unsteady. By comparing SMILE's X-ray-based observations with simultaneous solar wind observations, reconnection can be categorized as inherently unsteady or triggered by variations in the interplanetary magnetic field (IMF) (Sibeck et al., 2018). SMILE observations thus contribute to our understanding of magnetic reconnection, a fundamental heliophysics phenomenon. However, before SMILE observations of magnetopause and auroral oval motion and brightness variations can be attributed to reconnection, they must be distinguished from changes driven by solar wind dynamic pressure variations. The magnetopause does not move solely in response to variations in the IMF orientation; it also moves in response to variations in the solar wind pressure. Since SMILE takes its own observations of the solar wind plasma and IMF, it is a self-standing mission.

To help identify the cause of magnetopause and auroral motion,

Correspondence to: S-Y. W. Hsieh, Syau-Yun.Hsieh@jhuapl.edu
Received 06 DEC 2023; Accepted 26 DEC 2023.
First Published online 04 JAN 2024.

or auroral brightening, other data sets may be of use. In particular, magnetic field perturbations detected by both geosynchronous satellites and stations on the surface of the Earth at dayside equatorial latitudes have been associated with variations in solar wind dynamic pressure and IMF orientation (Gosling et al., 1967; Wilken et al., 1982). Increases in solar wind dynamic pressure are known to launch fast mode compressional waves when they strike the magnetopause. These waves propagate across magnetic field lines and enhance field strengths both in the magnetosphere and on Earth's surface. Southward IMF turnings initiate reconnection and launch fast rarefaction waves that propagate across magnetic field lines to depress dayside magnetospheric magnetic fields at geosynchronous orbit (Sibeck, 1994; Wing et al., 2002). One might expect the same fast rarefaction waves to reach the surface of the Earth and depress dayside equatorial magnetic field strengths, but that is not the prevailing consensus.

In pioneering papers, Nishida (1966; 1968a; b) employed arrays of ground magnetometers to identify global convection patterns distinctly different from those associated with substorm onset. Whereas substorm convection patterns are centered on nightside auroral electrojets, the newly detected convection patterns appear to extend both to lower latitudes and into the polar cap. Perturbations at high and low latitudes vary in phase. Most curiously of all, their northward (*H* or *N*) component, registered in dayside equatorial ground magnetograms, increases (not decreases) in response to southward IMF turnings.

It might be thought that the new convection pattern identified in correlated solar wind plasma and IMF changes has resulted from an accidental misassociation of solar wind pressure-driven ground-based perturbations with southward IMF turnings (Heppner, 1969). However, Nishida and Maezawa (1971) have estimated that global response times are longer for the new pattern than for pressure driven perturbations; they have presented several examples of ground-based perturbations associated with IMF variations that occurred in the absence of any solar wind pressure variation.

The proposed 'new' global convection pattern is not rare. In fact, it predominates. Nishida et al. (1966) identified 80 north/south (*H*) component perturbations with amplitudes greater than 40 nT during 270 hours of dayside Huancayo equatorial ground magnetometer observations between 1000 and 1300 local time. Signatures characteristic of the new global convection pattern were present in 60% of the hours examined and constituted 60 of the 80 identified perturbations. Of the remaining 20 perturbations, only one resulted from a solar flare; 19 could be associated with the sudden commencement of impulse signatures that indicate global magnetospheric compressions driven by pressure variations.

Studies of the response seen in dayside equatorial ground magnetograms continue to the present day. Of 56 perturbations seen over 12 months in equatorial ground magnetograms, Sibeck et al. (1998) ascribed a third to solar wind dynamic pressure variations, a third to a response to IMF B_z, and a third to nightside substorm onsets. Kikuchi et al. (1996, 2000, 2008) interpreted increases in the *H* component driven by southward IMF turnings to electric fields propagating down to the polar and auroral ionosphere and then promptly propagating to the equator through an ionosphere waveguide. More recently, Yizengaw et al. (2016) associated IMF variations with similar perturbations in dayside equatorial ground magnetograms, but did not present or discuss observations of corresponding (strong) solar wind dynamic pressure variations.

To determine the cause(s) of perturbations seen in dayside equatorial ground magnetograms, we present a systematic survey employing solar wind observations made simultaneously by instruments on geosynchronous satellites and at ground-based stations. This paper employs OMNIWeb observations lagged to the subsolar bow shock for the solar wind input. However, we cannot be sure that features seen far upstream at the L1 libration point actually arrive at Earth (Crooker et al., 1982). And even if they do, we now know that they can be greatly modified within the foreshock (Fairfield et al., 1990), or even within the quasi-perpendicular bow shock (Sibeck and Gosling, 1996), resulting in pressure perturbations that can sometimes compress the magnetosphere but also sometimes allow the magnetopause to expand far outside its nominal location (Merka et al., 2003; Suvorova et al., 2010). Hence, GOES geosynchronous magnetic field observations are essential to determine whether enhancements in the equatorial ionospheric magnetic field strength are associated with fast rarefaction waves at geosynchronous orbit (as expected by current models for southward IMF turnings) or with fast compressional waves at geosynchronous orbit (as expected for increases in the solar wind dynamic pressure). This paper presents results from such an initial study.

2. Data and Methods

We compared lagged OMNI solar wind plasma and magnetic field observations in GSM coordinates and flow pressure, with the total magnetic field strength from the geosynchronous GOES-16 and -17 spacecraft and from Huancayo, Peru ground magnetograms. The OMNI solar wind data are publicly accessible via OMNIWeb at 1-minute time resolution. CDAWeb provides high-resolution NOAA/GOES satellite data at 0.1-second time resolution. Both OMNIWeb and CDAWeb are web services provided by NASA's Space Physics Data Facility (SPDF) at Goddard Space Flight Center (GSFC). The 1-minute time resolution ground magnetograms from Huancayo station (Gjerloev, 2012), located at geographic (longitude, latitude) = (284.67°, −12.05°) and magnetic (longitude, latitude) = (−2.75°, 1.17°), are obtained via JHUAPL's SuperMAG, a web-based data service funded by U.S. National Science Foundation (NSF). Taking the same approach as Nishida, we chose a period of 90 days from December 1, 2020 to February 28, 2021. We examine data collected daily from 14:00:00 to 20:00:00 UT, because 17:00:00 is when Huancayo passes through local noon. GOES-16 and -17 pass through local noon at 17:00 and 21:00 UT each day.

To survey the data systematically and consistently, we use the criteria listed in Table 1 to identify perturbation events and investigate their causes. Our minimum requirement for a candidate event is an increase of 20 nT, for at least 6 minutes, in the north/south component of the ground magnetogram. We detrend both GOES and Huancayo data to aid in event categorization by calculating a 60-minute running average and subtracting this value from the point at the center of the averaging interval.

Table 1. Event classification criteria.

Model	Solar wind		Geosynchronous GOES	Ground magnetograms	Event duration
	IMF B_z	Pressure	Total B field	N component (N positive in local magnetic north direction)	Ground magnetograms
Nishida	Southward	Constant in clearest cases	Decrease	Minimum of 20 nT increase	6 minutes to 2 hours
Sibeck	Constant in clearest cases	Increase	Increase	Minimum of 20 nT increase	6 minutes to 2 hours

3. Results and Discussion

Figures 1–4 show representative events. From top to bottom, each figure shows lagged solar wind dynamic pressure, lagged IMF B_z, the detrended geosynchronous magnetic field strength, and the detrended north/south component of the Huancayo ground magnetograms. The time interval of each identified event is highlighted by two vertical orange-colored dashed-lines; a horizonal aquamarine-colored dashed-line shows the criterion 20 nT in detrended ground N component.

In Figure 1, these fields follow southward IMF turnings by 10–20 minutes at times when the solar wind dynamic pressure does not increase significantly. They do correspond to depressed geosynchronous magnetic field strengths. Consequently, these events are consistent with the model proposed by Nishida.

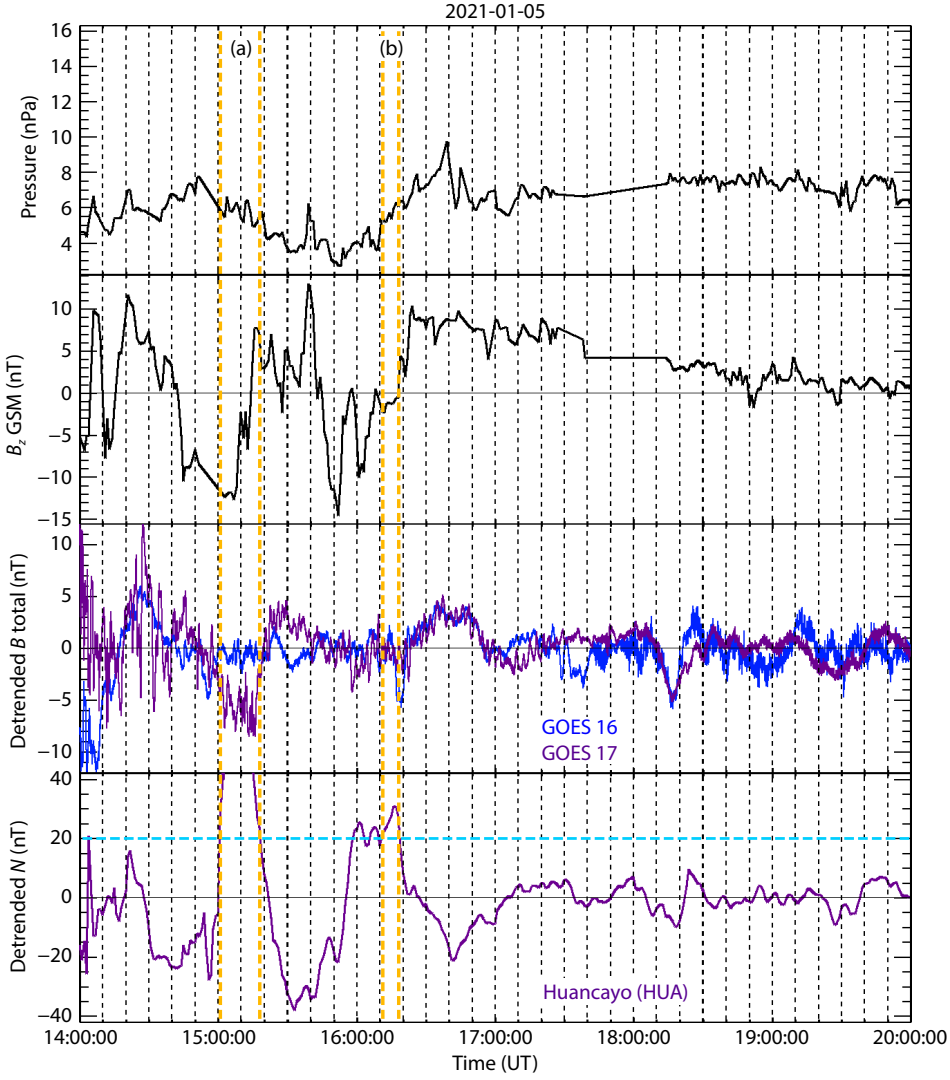

Figure 1. Two IMF B_z events supporting the Nishida model were identified on January 5, 2021: (a) 15:01:00–15:18:00 and (b) 16:11:00–16:18:00. In event (a), the detrended ground magnetic N component exhibits a significant increase greatly exceeding the 20 nT criterion for 18 minutes. By comparison, the N component increase in event (b) is much smaller than that of event (a) and lasts only for about 8 minutes. During both events, data from both GOES satellites show either a decreasing or relatively steady magnetic field. Solar wind IMF B_z data exhibit lags of approximately 10 and 20 minutes, respectively, in relation to the Huancayo detection times of events (a) and (b).

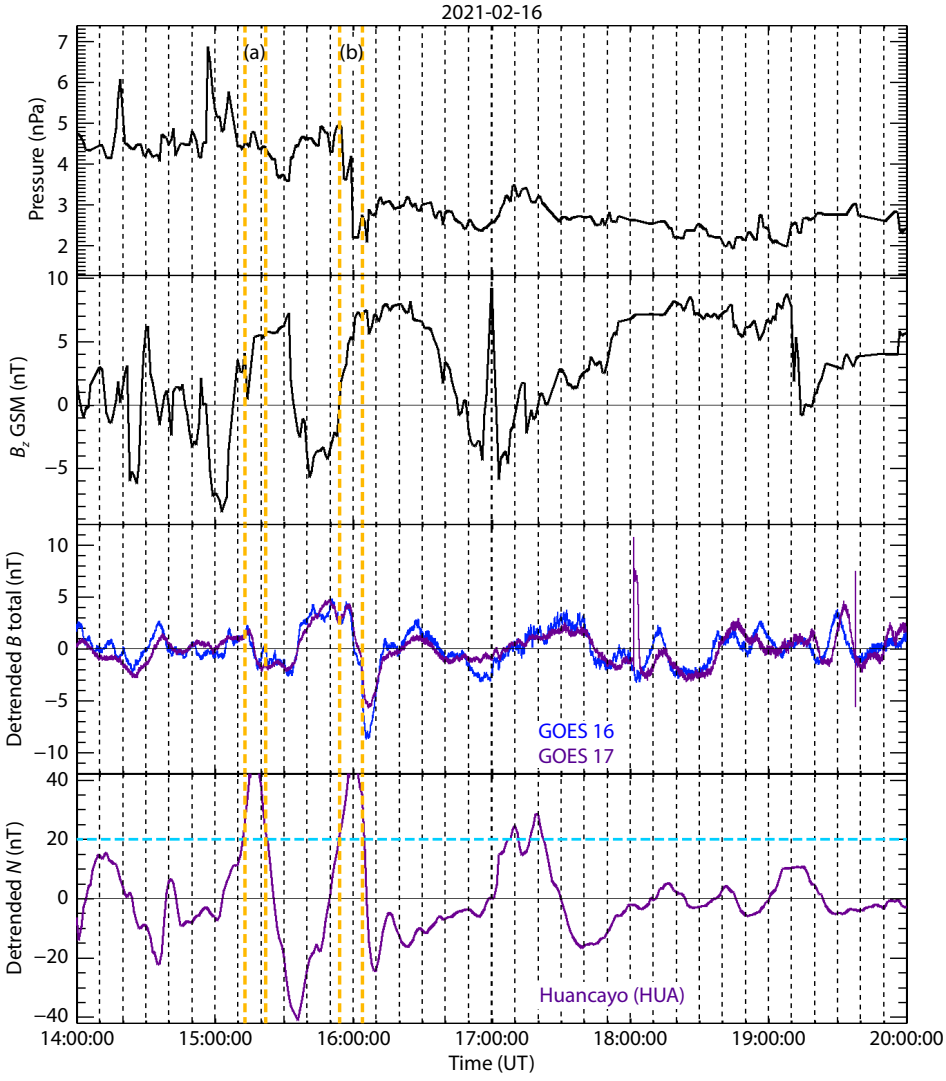

Figure 2. Two IMF B_z events were identified on February 16, 2021: (a) 15:13:00–15:22:00 and (b)15:54:00–16:04:00. Sharp increases greater than 20 nT are seen in the detrended ground magnetic N components lasting 10 and 11 minutes, respectively, for events (a) and (b). During both events, data from both GOES satellites show a decreasing magnetic field. Solar wind IMF B_z data exhibit a lag of about 15 minutes in both events. However, these two events could also fit the Pressure model.

In Figure 2, the northward perturbations at Huancayo follow southward IMF turnings (now by 15 minutes), and again occur at times when solar wind dynamic pressure is not significantly increasing. However, these events also follow solar wind dynamic pressure decreasing by 15 minutes. They correspond to decreasing geosynchronous magnetic field strengths. Thus these two events could be seen as consistent with either model.

In the single event presented in Figure 3, the northward perturbation at Huancayo and magnetic field strength increase at the GOES spacecrafts correspond directly to an unambiguous increase in the solar wind dynamic pressure. Moreover, the shapes of the ground- and geosynchronous perturbations differ from those of the events in Figures 1 and 2, associated with southward IMF B_z turnings. This Figure 3 event is most readily interpreted in terms of the pressure model.

Figure 4 presents several northward perturbations in the Huancayo ground magnetometers. The northward perturbations at 16:40:00–16:50:00 and 17:41:00–17:47:00 UT satisfy our identification criteria. Both they and other weaker/shorter duration perturbations in the ground magnetic field during the time interval of 16:00:00–19:30:00 UT correspond very well to increases in the solar wind dynamic pressure and compressions of the geosynchronous magnetic field, but not to southward IMF turnings. Consequently the perturbations on this day are most readily interpreted in terms of the pressure model.

Using the criteria in Table 1, we identified a total of 19 events, listed in Table 2, during the 90-day survey period — many fewer than the 80 identified by Nishida, in a corresponding 3-month period, using a different perturbation amplitude criterion. We categorize these 19 events as follows: 7 pressure events, 6 IMF B_z events, 4 events that can be either pressure events or IMF B_z events with ~15–20-minute lags, 1 event that both models did not fit, and 1 event that lacked sufficient solar wind data to meet our criteria for evaluation. These results suggest that pressure-

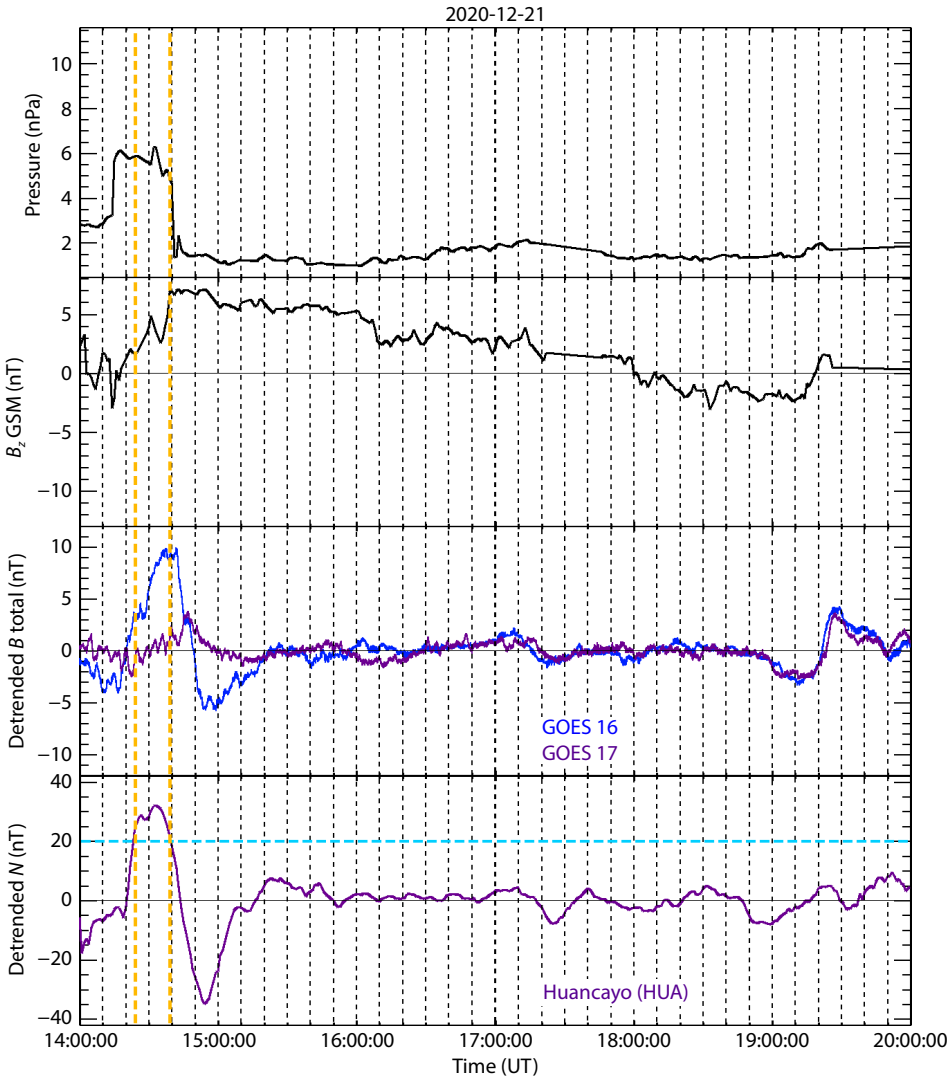

Figure 3. One pressure event supporting the Sibeck model was identified in 14:24:00–14:39:00 on December 21, 2020. A sizeable increase to more than 20 nT appears in the detrended ground magnetic *N* component; the increase persists for about ~16 minutes. Both GOES satellites registered a corresponding magnetic field increase. A significant increase, including a sharp pulse, occurs in the solar wind pressure.

and IMF B_z-related events are approximately equally common; that IMF B_z does not dominate.

Note that nearly all the IMF B_z events identified in this 90-day period required lag times from the solar wind monitor to the bow shock that are greater than that given by OMNIWeb. These lags generally range from 10 to 20 minutes, consistent with Yu YQ and Ridley (2009a). By contrast, the pressure variation events generally exhibit lags ranging from 0 to several minutes, consistent with Yu YQ and Ridley (2009b). While it is possible that the longer lags reported here for the IMF B_z events result from poor estimates of the lag times from the solar wind monitor to Earth, it seems more likely that they result from the time required for reconnection and enhanced magnetospheric convection to be established. Past work indicates that the durations of the growth phase of geomagnetic substorms following southward IMF turnings range from 20 to 160 minutes, but are typically on the order of ~71 minutes (e.g., Li H et al., 2013). Consequently, we expect peak perturbations in equatorial ground magnetograms to follow the arrival of southward IMF turnings by several tens of minutes.

4. Conclusions

We have completed an initial survey of observations of dayside equatorial magnetic field at a ground station, correlated with corresponding satellite observations of solar wind and geosynchronous magnetic field values, during for a selected 90-day time period. Significant field perturbations detected at the ground station were identified and related to relevant IMF B_z and solar wind pressure data. Our analysis suggests that the numbers of identified events attributable to the IMF B_z and pressure variation models are nearly equal. Geosynchronous magnetic field observations are a useful, perhaps essential, tool in distinguishing between the two proposed causal mechanisms. Future studies will address seasonal variations, patterns of occurrence of weaker events, relationships to substorm onset, and the spatial extent of perturbations in equatorial magnetograms. Such studies will be able to make use of improved near-earth solar wind observations just upstream from the bow shock to reduce uncertainties in solar wind input. To determine the extent of the ground perturbations, they will also benefit from data collected by the extensive array of

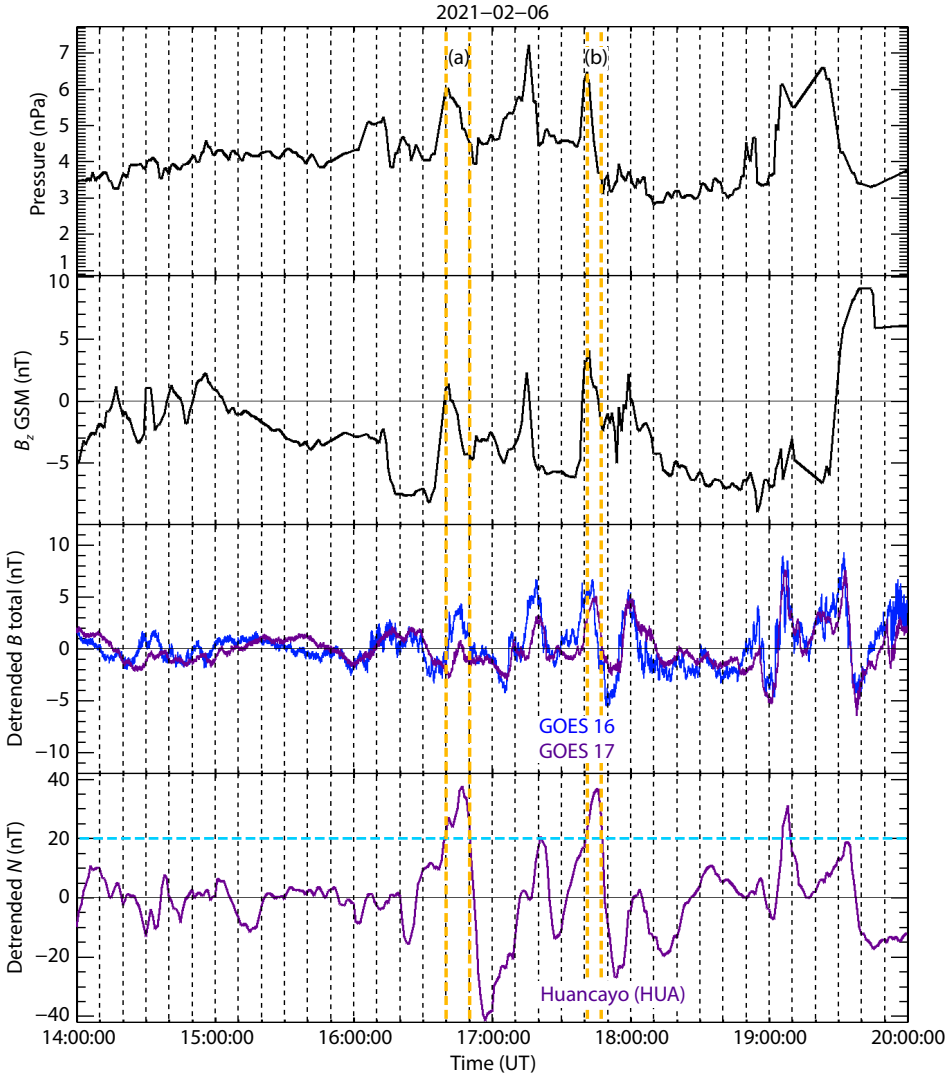

Figure 4. Two pressure events supporting the Sibeck model were identified on February 6, 2021: (a) 16:40:00–16:50:00 and (b) 17:41:00–17:47:00. Sharp increases greater than 20 nT appear in the detrended ground magnetic *N* component lasting 11 and 7 minutes, respectively, for events (a) and (b). During both events, a sharp increase was observed in solar wind pressure; an increase in magnetic field was observed from both GOES satellites.

ground magnetometers in Brazil.

Acknowledgments

The authors thank the SMILE mission and SMILE Modeling Working Group (MWG) for organizing and supporting this SMILE special issue. The authors want to express our gratitude to the support of the editor and reviewers. We are very grateful to the SPDF of NASA/GSFC for providing access to the OMNI solar wind and high-resolution geosynchronous NOAA GOES data sets. The authors are also very grateful to JHUAPL's SuperMag data service for proving the 1-min-resolution ground magnetograms from Huancayo station. This work was supported by NASA grant 80NSSC23K1241.

References

Branduardi-Raymont, G., Wang, C., Escoubet, C. P., Adamovic, M., Agnolon, D., Berthomier, M., Carter, J. A., Chen, W., Colangeli, L., … Zhu, Z. (2018). SMILE definition study report. European Space Agency. https://doi.org/10.5270/esa.smile.definition_study_report-2018-12

Branduardi-Raymont, G., and Wang, C. (2022). The SMILE mission. In C. Bambi, et al. (Eds.), *Handbook of X-ray and Gamma-ray Astrophysics* (pp. 1-22). Singapore: Springer. https://doi.org/10.1007/978-981-16-4544-0_39-1

Crooker, N. U., Siscoe, G. L., Russell, C. T., and Smith, E. J. (1982). Factors controlling degree of correlation between ISEE 1 and ISEE 3 interplanetary magnetic field measurements. *J. Geophys. Res.: Space Phys.*, *87*(A4), 2224–2230. https://doi.org/10.1029/JA087iA04p02224

Fairfield, D. H., Baumjohann, W., Paschmann, G., Lühr, H., and Sibeck, D. G. (1990). Upstream pressure variations associated with the bow shock and their effects on the magnetosphere. *J. Geophys. Res.: Space Phys.*, *95*(A4), 3773–3786. https://doi.org/10.1029/JA095iA04p03773

Gjerloev, J. W. (2012). The SuperMAG data processing technique. *J. Geophys. Res.: Space Phys.*, *117*(A9), A09213. https://doi.org/10.1029/2012JA017683

Gosling, J. T., Asbridge, J. R., Bame, S. J., Hundhausen, A. J., and Strong, I. B. (1967). Measurements of the interplanetary solar wind during the large geomagnetic storm of April 17-18, 1965. *J. Geophys. Res.*, *72*(7), 1813–1821. https://doi.org/10.1029/JZ072i007p01813

Heppner, J. P. (1969). Magnetospheric convection patterns inferred from high latitude activity. In B. M. McCormac, et al. (Eds.), *Atmospheric Emissions* (pp. 251-266). New York: Van Nostrand Reinhold.

Kikuchi, T., Lühr, H., Kitamura, T., Saka, O., and Schlegel, K. (1996). Direct

Table 2. Events Identified during a 90-day survey period (December 2020 – February 2021).

Date	Time period	Event type
2020-12-09	18:40:00–18:47:00	Pressure
2020-12-21	14:24:00–14:39:00	Pressure
2020-12-28	14:02:00–14:10:00	No evaluation due to data gaps in solar wind data
2021-01-05	15:01:00–15:18:00	IMF B_z with a ~10-minute lag
2021-01-05	16:11:00–16:18:00	IMF B_z with a ~20-minute lag
2021-01-11	14:45:00–14:50:00	IMF B_z with a ~8-minute lag
2021-01-11	15:13:00–15:24:00	IMF B_z with a ~20-minute lag or pressure
2021-01-11	15:59:00–16:19:00	IMF B_z with a ~22-minute lag
2021-01-11	16:47:00–17:01:00	IMF B_z with a ~15-minute lag or pressure
2021-01-11	19:52:00–19:58:00	IMF B_z with a ~11-minute lag
2021-01-25	16:30:00–16:39:00	Neither
2021-01-26	17:18:00–17:23:00	Pressure
2021-01-26	18:08:00–18:13:00	IMF B_z with a ~10-minute lag
2021-02-06	16:40:00–16:50:00	Pressure
2021-02-06	17:41:00–17:47:00	Pressure
2021-02-16	15:13:00–15:22:00	IMF B_z with a ~15-minute lag or pressure
2021-02-16	15:54:00–16:04:00	IMF B_z with a ~15-minute lag or pressure
2021-02-16	17:17:00–17:22:00	Pressure
2021-02-26	18:04:00–18:12:00	Pressure

penetration of the polar electric field to the equator during a *DP* 2 event as detected by the auroral and equatorial magnetometer chains and the EISCAT radar. *J. Geophys. Res.: Space Phys.*, *101*(A8), 17161–17173. https://doi.org/10.1029/96JA01299

Kikuchi, T., Lühr, H., Schlegel, K., Tachihara, H., Shinohara, M., and Kitamura, T. I. (2000). Penetration of auroral electric fields to the equator during a substorm. *J. Geophys. Res.: Space Phys.*, *105*(A10), 23251–23261. https://doi.org/10.1029/2000JA900016

Kikuchi, T., Hashimoto, K. K., and Nozaki, K. (2008). Penetration of magnetospheric electric fields to the equator during a geomagnetic storm. *J. Geophys. Res.: Space Phys.*, *113*(A6), A06214. https://doi.org/10.1029/2007JA012628

Li, H., Wang, C., and Peng, Z. (2013). Solar wind impacts on growth phase duration and substorm intensity: a statistical approach. *J. Geophys. Res.: Space Phys.*, *118*(7), 4270–4278. https://doi.org/10.1002/jgra.50399

Merka, J., Szabo, A., Šafránková, J., and Němeček, Z. (2003). Earth's bow shock and magnetopause in the case of a field-aligned upstream flow: observation and model comparison. *J. Geophys. Res.: Space Phys.*, *108*(A7), 1269. https://doi.org/10.1029/2002JA009697

Nishida, A., Iwasaki, N., and Nagata, T. (1966). The origin of fluctuations in the equatorial electrojet: a new type of geomagnetic variation. *Ann. Geophys.*, *22*(3), 478–484.

Nishida, A. (1968a). Geomagnetic D_p 2 fluctuations and associated magnetospheric phenomena. *J. Geophys. Res.*, *73*(5), 1795–1803. https://doi.org/10.1029/JA073i005p01795

Nishida, A. (1968b). Coheence of geomagnetic *DP* 2 fluctuations with interplanetary magnetic variations. *J. Geophys. Res.*, *73*(17), 5549–5559. https://doi.org/10.1029/JA073i017p05549

Nishida, A., and Maezawa, K. (1971). Two basic modes of interaction between the solar wind and the magnetosphere. *J. Geophys. Res.*, *76*(10), 2254–2264. https://doi.org/10.1029/JA076i010p02254

Sibeck, D. G. (1994). Signatures of flux erosion from the dayside magnetosphere. *J. Geophys. Res.: Space Phys.*, *99*(A5), 8513–8529. https://doi.org/10.1029/93JA03298

Sibeck, D. G., and Gosling, J. T. (1996). Magnetosheath density fluctuations and magnetopause motion. *J. Geophys. Res.: Space Phys.*, *101*(A1), 31–40. https://doi.org/10.1029/95JA03141

Sibeck, D. G., Takahashi, K., Yumoto, K., and Reeves, G. D. (1998). Concerning the origin of signatures in dayside equatorial ground magnetograms. *J. Geophys. Res.: Space Phys.*, *103*(A4), 6763–6769. https://doi.org/10.1029/97JA03600

Sibeck, D. G., Allen, R., Aryan, H., Bodewits, D., Brandt, P., Branduardi-Raymont, G., Brown, G., Carter, J. A., Collado-Vega, Y. M., … Wing, S. (2018). Imaging plasma density structures in the soft X-rays generated by solar wind charge exchange with neutrals. *Space Sci. Rev.*, *214*(4), 79. https://doi.org/10.1007/s11214-018-0504-7

Suvorova, A. V., Shue, J. H., Dmitriev, A. V., Sibeck, D. G., McFadden, J. P., Hasegawa, H., Ackerson, K., Jelínek, K., Šafránková, J., and Němeček, Z. (2010). Magnetopause expansions for quasi-radial interplanetary magnetic field: THEMIS and Geotail observations. *J. Geophys. Res.: Space Phys.*, *115*(A10), A10216. https://doi.org/10.1029/2010JA015404

Wilken, B., Goertz, C. K., Baker, D. N., Higbie, P. R., and Fritz, T. A. (1982). The SSC on July 29, 1977 and its propagation within the magnetosphere. *J. Geophys. Res.: Space Phys.*, *87*(A8), 5901–5910. https://doi.org/10.1029/JA087iA08p05901

Wing, S., Sibeck, D. G., Wiltberger, M., and Singer, H. (2002). Geosynchronous magnetic field temporal response to solar wind and IMF variations. *J. Geophys. Res.: Space Phys.*, *107*(A8), 1222. https://doi.org/10.1029/2001JA009156

Yizengaw, E., Moldwin, M. B., Zesta, E., Magoun, M., Pradipta, R., Biouele, C. M., Rabiu, A. B., Obrou, O. K., Bamba, Z., and de Paula, E. R. (2016). Response of the equatorial ionosphere to the geomagnetic *DP* 2 current system. *Geophys. Res. Lett.*, *43*(14), 7364–7372. https://doi.org/10.1002/2016GL070090

Yu, Y. Q., and Ridley, A. J. (2009a). Response of the magnetosphere-ionosphere system to a sudden southward turning of interplanetary magnetic field. *J. Geophys. Res.: Space Phys.*, *114*(A3), A03216. https://doi.org/10.1029/2008JA013292

Yu, Y. Q., and Ridley, A. J. (2009b). The response of the magnetosphere-ionosphere system to a sudden dynamic pressure enhancement under southward IMF conditions. *Ann. Geophys.*, *27*(12), 4391–4407. https://doi.org/10.5194/angeo-27-4391-2009